

Selecting long-lived particles in the first trigger level at the LHC

Lorenzo Pica* for the LHCb collaboration

*INFN Sezione di Pisa,
Largo Bruno Pontecorvo 3, Pisa, Italy
Scuola Normale Superiore,
Piazza dei Cavalieri 7, Pisa, Italy
E-mail: lorenzo.pica@cern.ch*

The LHCb experiment is starting to take data in Run 3 with a new DAQ system, capable of performing complete event reconstruction at the full LHC collision rate. One novel opportunity offered by this system is triggering on long-lived particles (LLPs) at the very first stage of the trigger. This could potentially increase trigger efficiency for LLPs, typically suffering from low online detection efficiency at hadron collider experiments, because of their decay signatures. We investigated the feasibility and effectiveness of an early LLP-triggering approach in LHCb with the implementation of two LLP-dedicated selections in the first trigger level (HLT1), targeting the presence of either one, or two, K_S^0 decays. Selection tuning is performed on simulation, targeting some benchmark channels with K_S^0 particles in the final state, as $D^0 \rightarrow K_S^0 K_S^0$ and $B^0 \rightarrow K_S^0 K_S^0$. Tests ran on simulated samples predict a large increase in selection efficiency, up to 2.6x for the $D^0 \rightarrow K_S^0 K_S^0$ channel, at the price of a very modest increase of HLT1 computational load and trigger rate. These selections were implemented in the GPU-based HLT1 trigger sequence, and took data during the physics data-taking LHCb run in year 2022. In this document, we present results obtained from these first data, yielding good quality K_S^0 and K_S^0 -pair samples even from a very limited integrated luminosity. We conclude with a discussion of the physics prospects opened by these new triggers, and their planned extension to tracks decaying outside the volume of the VELO subdetector ("downstream tracks") to further extend their acceptance.

*Corfu2023 Workshop on Future Accelerators
23-29 April 2023
Faliraki, Old town Corfu, Greece*

*Speaker

Contents

1	LLP scenario	2
1.1	Beyond Standard Model LLPs physics case	3
1.2	Standard Model LLPs physics case	3
1.3	LLPs study at the LHC	4
1.4	LLP triggering	4
2	LLP triggering at LHCb	5
2.1	Track reconstruction in LHCb	5
2.2	The LHCb trigger architecture	6
2.3	New trigger lines	6
2.3.1	Novel lines design and simulation studies	6
3	Initial commissioning	8
3.1	Candidate invariant mass distributions	8
3.2	Rates on real pp collisions	9
4	Possible acceptance extension	10
4.1	HLT1 downstream triggering potential	10
4.2	Downstream tracking efforts	11
5	Conclusions	12

1. LLP scenario

Many measurements in High Energy Physics (HEP) involve particles decaying with extremely short flight distances, as the electroweak bosons W^\pm/Z^0 and the Higgs boson H^0 . *Beauty* and *charm* hadrons have longer lifetimes ($\tau \sim 10^{-12}$ s), but their flight distance is still limited to few mm, even in multi-TeV collisions. This common feature drove the design of most general-purpose experiments, aimed at detection and selection of short-lived states. However, particles with longer flight distances, up to hundreds of centimeters, usually referred to as long-lived particles (LLPs) are also involved in a large number of interesting processes.

In many cases, the sensitivity of measurements involving LLPs suffers of specific experimental limitations related to their long flight paths. In particular, at hadron colliders one of the important issues is the difficulty of achieving a good efficiency in the online selection of such events. However, the advent of full-event reconstruction in real time opens new possibilities also in this respect. In this work, I will show that it can be exploited to significantly increase the LLP online selection efficiency at LHCb. Before going through this, it is worth mentioning some notable LLP measurements, motivating these efforts.

1.1 Beyond Standard Model LLPs physics case

Among the particles predicted by BSM theories, several have a large lifetime, because of the very small coupling between BSM state and detectable SM particles, or a reduced available phase space for the BSM particle decay. The search for such LLPs is therefore of extreme interest, since any detection would be an evidence of BSM physics.

Supersymmetry (SUSY) is still one of the most interesting BSM frameworks. It predicts the existence of a supersymmetric partner for every SM particle and some of these are expected to have a large lifetime, behaving experimentally as LLPs. Searches for these have been extensively performed and taking the ATLAS collaboration as an example, several decay signatures have been analyzed: fully-hadronic displaced vertex with an associated muon [1], a single high-impact-parameter lepton [2], displaced vertices when collisions are absent [3], so-called *disappearing tracks* [4], or multi-charged particles [5].

A possible production mode for BSM particles is through the decay of an Higgs boson (the so-called Higgs portal). This process is particularly interesting as it is allowed by the current knowledge on the Higgs boson total decay width, possibly including decays into unknown objects with branching fractions up to 30% [6]. Searches have been performed by different collaborations, as D0 [7], CDF [8], ATLAS [9], CMS [10] and LHCb [11]. Taking as example the latest LHCb result, a search is performed for the hidden sector lightest state π_ν , exploiting 2 fb^{-1} of data collected during Run 1 of LHC. Considered mass and lifetime hypothesis lay in the $25 - 50 \text{ GeV}/c^2$ and $2 - 500 \text{ ps}$ ranges, respectively. The presence of a displaced vertex having transverse distance from beam axis R_{xy} larger than 0.4 mm and two associated hadronic jets is required during online selection. No evidence has been found for π_ν during analysis and upper limits on the cross section are set.

Heavy neutral leptons (HNLs) are another example of BSM LLPs. These are heavy counterparts of SM neutrinos by the so-called Seesaw mechanism [12–14], with their mass upper end being $O(\text{TeV}/c^2)$. Several searches for HNLs have been performed and an extensive review can be found in Ref. [15]. An interesting example is the HNLs search recently published by CMS collaboration, based on the full statistics collected during Run 2 of the LHC (138 fb^{-1}) [16]. Here the presence of three leptons in the final state is required - one coming from the primary proton-proton interaction, and the others forming a displaced secondary vertex within the CMS tracking system. No evidence for BSM decays is found and upper limits are set on the mixing probability between SM and BSM neutrinos.

Many other BSM theories predict the existence of LLPs, detectable in current and future experiments, as dark photons [17] or axion-like particles [18] – it is beyond the scope of this document to discuss all of them. The examples mentioned should be sufficient to convey the richness of BSM physics accessible through LLPs.

1.2 Standard Model LLPs physics case

SM LLPs play a crucial role in current SM experimental physics as well. They give access to a large number of interesting measurement and, additionally, they offer a perfect ground for developing and testing LLPs-specific experimental techniques. They are abundantly produced and detected already in present experiments, with strange particles K_S^0 and Λ making the most common examples.

The measurement of the $K_S^0 \rightarrow \mu^+ \mu^-$ decay branching ratio is an outstanding example of the impact of measurements involving SM LLPs. A precise knowledge of this parameter is interesting because of the very small value of the SM prediction, being 5×10^{-12} [19], and making it an excellent null test for the SM, sensitive to new physics influence. $\text{BR}(K_S^0 \rightarrow \mu^+ \mu^-)$ has been measured several times, and LHCb published the best and most recent result [20], exploiting data collected during Run 2 of the LHC (5.6 fb^{-1}). Despite the huge amount of produced K_S^0 mesons, no evidence for this decay has been found, and an upper limit is set to $\text{BR}(K_S^0 \rightarrow \mu^+ \mu^-) < 2.1 \times 10^{-10}$ at 90% CL [20].

CP violation (CPV) in *charm* decays is another phenomenon that can be investigated through the study of K_S^0 . It has been observed for the first time by LHCb collaboration in 2019 [21], analyzing $D^0 \rightarrow K^+ K^-$ and $D^0 \rightarrow \pi^+ \pi^-$ decays. However, agreement with the theory can't currently be determined, because of predictions precision level. The observation of additional charm CPV manifestation can improve experimental precision and provide a crucial input to theory. $D^0 \rightarrow K_S^0 K_S^0$ represent an excellent candidate for a charm CPV confirmation, since its time-integrated CPV size could be enhanced up to 1.1% [22]. Several measurements of $\mathcal{A}^{CP}(D^0 \rightarrow K_S^0 K_S^0)$ has been performed [23–26], and thanks to the most recent LHCb result [26] world average approached theoretical predictions upper end for the first time, strongly motivating the collection of additional statistics.

Also the system of beauty neutral mesons offer an important measurement when LLPs are involved, with the $B^0 \rightarrow J/\psi K_S^0$ decay, providing a theoretically clean access to the CKM angle β [27, 28] through the measurement of its CPV parameters. Several measurements have been performed [29–31] and with the current precision no tension has been found in the determination of the CKM angles, motivating a more precise β determination.

1.3 LLPs study at the LHC

LLPs measurements are performed at different experiments and facilities. Results from ATLAS, CMS, LHCb, BaBar, and Belle have been reported, but also other are involved in LLPs study, as non-accelerators ones (IceCube [32] and Super-Kamiokande [33]) or LLP-dedicated experiments, both present (NA62 [34]) and future ones (CODEX-b [35] and FASER [36]). In this wide scenario the Large Hadron Collider is one of the most suitable facilities for the study of LLPs. In fact, thanks to the very large cross section provided by hadron collisions, it allows the collection of huge samples in a very short timescale, with the most advanced HEP detectors recording produced collisions. Additionally, LHC, and CERN in general, can profit from an almost-unique decade-long timescale for their facilities and projects, as stated in the last update of the European Strategy for Particle Physics [37].

However, the large LLP production rate made available by the LHC is just the first step toward the collection of the large statistics required to achieve high-precision measurements. In fact, in order to be exploited for offline analyses, LLPs need to be identified in real time and saved to permanent storage. This task is fulfilled by the so-called *trigger* algorithm, performing real-time selection of interesting processes.

1.4 LLP triggering

Triggering is an extremely challenging task at the LHC, because of the very crowded environment of hadron collisions and the very small time window in which the algorithm has to operate.

Because of these tight constraints, signal identification is usually based on very distinctive signatures, as a large transverse momentum/energy deposit. These provide an effective handle for signal identification and are also accessible with the exploitation of fastest sub-detectors, as calorimetric and muon systems.

However, this strategy has a limited performance when applied to LLPs decays, being their typical decay signatures displaced tracks and vertices, characterized by a relatively low p_T , significantly different from the ones of prompt objects. The implementation of a dedicated trigger strategy is extremely challenging, since the identification of such signatures requires a series of computationally heavy tasks, as tracking systems read-out and tracks and vertices reconstruction. Because of this, LLP-dedicated triggers are typically implemented only in later stages of the trigger, when more processing time is available. However, this condition strongly limits the efficiency achievable in the early stages of the trigger, where LLP decays were retained only when an unrelated process randomly fired the trigger. It can therefore be expected that if the LLPs selection could be moved to earlier stages of the trigger, their online selection efficiency could improve significantly. LHCb, with the implementation of its upgraded detector and DAQ system, is a very suitable LHC experiment for attempting this.

2. LLP triggering at LHCb

LHCb is a forward single-arm spectrometer, specifically designed to study *beauty* and *charm* hadron decays. It profits from an excellent momentum resolution and vertex identification precision with its tracking system [38], $\pi/K/p$ separation with its Particle IDentification system (PID) [38] and muon identification through a dedicated sub-detector [38]. Its acceptance covers the $2 < \eta < 5$ range¹, making it complementary to other LHC major experiments. LHCb went under a major upgrade during the long shutdown 2 of the LHC (so-called Upgrade I [38]) that has seen the complete replacement of its entire tracking, DAQ and trigger systems. The aim is to achieve real time reconstruction of tracks and vertices at the full LHC bunch-crossing rate.

2.1 Track reconstruction in LHCb

The upgraded LHCb tracking system is composed of three sub-detectors. The VERtex LOcator (VELO) is a silicon pixel detector, providing precise track and vertex reconstruction. The Upstream Tracker (UT) is an additional silicon detector placed upstream the magnet, speeding up event reconstruction and reducing fake tracks reconstruction rate. The Scintillating Fibre (SciFi) is placed downstream the magnet and allows the measurement of particles momentum.

Particle trajectories (*tracks*) can be reconstructed inside the LHCb detector with the entire tracking system, or just a part of it, and are classified as:

- **Long tracks**, reconstructed exploiting VELO, UT and SciFi - these offer the best resolution;
- **Downstream tracks**, reconstructed exploiting UT and SciFi only - these offer a worse resolution, but a larger acceptance for LLP decays;
- **T-tracks**, reconstructed exploiting SciFi hits only.

¹Pseudorapidity η , defined as $-\log(\tan(\theta/2))$, where θ is the angle between the beams flight direction and the momentum of the particle.

2.2 The LHCb trigger architecture

LHCb employs a fully software-based trigger system in Run 3, made of two subsequent steps, named HLT1 and HLT2. It implements a trigger-less readout of the entire tracking, calorimetric and muon detectors. HLT1 is designed to perform an event rate reduction of a factor of 30, with an output event rate of 1 MHz. This is achieved running a 30 MHz read-out and reconstruction of tracks and vertices.

This innovative approach enables the implementation of LLPs trigger selections at the earliest stage of the trigger, a first time ever at an hadron collider. This possibility has been investigated, designing HLT1 LLP-dedicated selections, in order to understand their sustainability in term of throughput and background rejection and the potential achievable efficiency gain. Only objects decaying within VELO acceptance will be considered at this stage, since only long tracks are reconstructed in the HLT1 design configuration.

2.3 New trigger lines

Given the novelty and complexity of this task, K_S^0 decays have been chosen as targets of novel selections, in order to work with a particle whose behavior is well-known and easily reproducible on simulation. Additionally, since K_S^0 mesons are hugely produced in LHC collisions, any commissioning operation of novel selections would be significantly simplified and sped up.

Two different selections (*trigger lines*) have been designed and implemented. *TwoTrackKs* targets single K_S^0 candidates and *TwoKs* selects K_S^0 candidates pairs, without any requirement on the parent particle. Lines are based on a set of rectangular selections. The exploitation of any classifier is excluded, in order to avoid the introduction of any correlation between exploited variables, potentially limiting precision on performed measurements. Additionally, this approach provides an easier understanding of selection impact, crucial in a commissioning phase.

2.3.1 Novel lines design and simulation studies

The computational cost of any new HLT1 algorithm must be carefully guarded, in order to maintain the required 30 MHz processing frequency. The novel lines we introduced satisfy this, having almost no impact on HLT1 throughput by design. In fact, displaced vertices reconstruction is run independently from K_S^0 -dedicated lines, and it anyway represents just a small fraction of overall timing ($O(\%)$), and *TwoKs* line does not require any additional vertex reconstruction, since no selection is applied on K_S^0 parent.

Any novel HLT1 selection must also achieve high acceptance on target decays while maintaining an excellent background rejection, since output bandwidth is almost fully allocated for the selection of heavy flavor decays [39]. In order to meet such tight requirements, thresholds has been tuned exploiting the TMVA rectangular cuts optimizer [40]. K_S^0 candidates present in a $D^0 \rightarrow K_S^0 K_S^0$ simulated sample have been adopted as signal sample. Any two-track combination with an invariant mass within $\pm 70 \text{ MeV}/c^2$ from $m(K_S^0)$ present in a simulated sample of generic pp collisions (*minimum bias*) has been adopted as background sample. Variables exploited in the selections are:

- χ^2/ndf : χ^2 obtained from the fit of a track reconstructed in the detector, normalized to its degrees of freedom;

- p/p_T : momentum/transverse momentum of the particle;
- *Impact Parameter (IP)*: distance of closest approach between the PV and the direction identified by the momentum of the particle;
- χ_{IP}^2 : difference between χ^2 obtained from PV fitting including a particle in the fit or not;
- χ_{vtx}^2/ndf : χ^2 of tracks origin vertex fit, normalized to its degrees of freedom;
- θ_{DIRA} : angle between the momentum of a particle and the direction identified by the PV and the decay vertex of that particle;
- $\theta_{\pi\pi}$ (*direction angle*): angle between the two particles forming the a decay vertex;
- IP combination: $IP(\pi^+) \times IP(\pi^-)/IP(K_S^0)$ ratio between daughters IP product and parent IP.

However, only selections on $\chi_{IP}^2(\pi)$, $p_T(\pi)$, $p(\pi)$, $p_T(K_S^0)$ and IP combination have been numerically optimized to achieve maximum signal/background separation, while remaining are kept fixed during optimization. These have been set following a different rationale, as ensuring a correct background shape identification in $m(\pi^+\pi^-)$ sidebands, or avoiding the application of a too tight selection in case of data/simulation disagreement for $\chi_{vtx}^2(K_S^0)$, $\cos(\theta_{DIRA})$ or $\cos(\theta_{\pi\pi})$ (especially during commissioning phases).

Selections defining TwoTrackKs and TwoKs lines are reported in Table 1. Specific K_S^0 signa-

Variable	TwoTrackKs selection	TwoKs selection
χ^2/ndf	< 2.5	< 2.5
$\chi_{IP}^2(\pi)$	> 50	> 15
$p_T(\pi)$	$> 470 \text{ MeV}/c$	$> 425 \text{ MeV}/c$
$p(\pi)$	$> 5 \text{ GeV}/c$	$> 3 \text{ GeV}/c$
$ m(\pi^+\pi^-) - m(K_S^0) $	$< 45 \text{ MeV}/c^2$	$< 45 \text{ MeV}/c^2$
$\chi_{vtx}^2(K_S^0)$	< 20	< 20
$\eta(K_S^0)$	$2 < \eta(K_S^0) < 4.2$	$2 < \eta(K_S^0) < 4.2$
$p_T(K_S^0)$	$> 2500 \text{ MeV}/c$	$> 1150 \text{ MeV}/c$
$\cos(\theta_{DIRA})$	> 0.99	> 0.99
$\cos(\theta_{\pi\pi})$	> 0.99	> 0.99
$\frac{IP(\pi^+) \times IP(\pi^-)}{IP(K_S^0)}$	$> 0.72 \text{ mm}$	$> 0.23 \text{ mm}$

Table 1: Selections applied by TwoTrackKs and TwoKs HLT1 line. In case of TwoKs line two K_S^0 candidates satisfying reported selections are required in the same event.

tures are exploited to keep background acceptance under control, as the specific invariant mass and a significant π displacement, while other are loosened to increase efficiency, as $p_T(\pi)$. TwoKs line applies lower thresholds for single K_S^0 candidate since requirement for a candidates pair reduces background acceptance.

The impact of the new lines on the HLT1 background acceptance has been estimated with the variation of HLT1 *rate*, hence HLT1 output rate when processing a 30 MHz minimum bias input. TwoTrackKs and TwoKs respectively determine a 40 kHz and 11 kHz increase of the overall HLT1 rate, corresponding to a variation limited to 4% and 1.1%.

The efficiency has been evaluated over a set of representative decays. It is computed as the ratio between the number of decays retained by a line and the total number of decays whose final state tracks can be reconstructed through long tracks. The TwoTrackKs line determines the most significant gain in case of $D^0 \rightarrow K_S^0 K_S^0$ decays, where HLT1 efficiency increases by a factor of 2.6. Other decay channels benefit from its introduction as well, as a 20% increase is estimated in case of $B^0 \rightarrow K_S^0 K_S^0$ (reaching 77%) and a 45% gain is estimated for $B^0 \rightarrow K_S^0 \pi^0$. TwoKs line shows an efficiency on $D^0/B^0 \rightarrow K_S^0 K_S^0$ decays larger than general-purpose track-based lines (that occupy more than 80% of the HLT1 output bandwidth). However, it shows a lower efficiency w.r.t. TwoTrackKs, despite looser thresholds. This is expected, since the minimum $p_T(\pi)$ required for a track in order to be reconstructed in HLT1, determines a tighter selection when four tracks are requested in the final state.

3. Initial commissioning

Performances estimated on simulation motivated TwoTrackKs and TwoKs lines implementation in the HLT1 system, allowing their exploitation at the start of Run 3 data taking, in 2022. Data collected during this phase allowed a crucial early commissioning of novel lines, even if collected during a commissioning phase of detector and trigger system. This is essential in order to take prompt action against any deviation from expected performances.

Lines performance on real data has been investigated analyzing a small sub-sample of 2022 data, corresponding to an integrated luminosity of 240 nb^{-1} .

3.1 Candidate invariant mass distributions

The first performed check is the inspection of K_S^0 candidates invariant mass distribution, reported in Figure 1 for the TwoTrackKs line. A peak is clearly present, centered around the known $m(K_S^0)$, with a gaussian shape and a very modest background contribution.

The 2D K_S^0 candidates invariant mass distribution for candidates collected by TwoKs line is reported in Figure 2. Clear evidence for a peak due to real K_S^0 pairs is present in this case as well, centered around $m(K_S^0)$ for both candidates. TwoKs line collected $\sim 2.5\text{k}$ candidates, $\sim 25\%$ of which are contained in the peak.

Considered distributions show how novel HLT1 lines successfully selected a sizeable sample of K_S^0 candidates and K_S^0 candidate pairs in pp collisions at the full LHC crossing rate of 30 MHz, a result never achieved before at an hadron collider.

It has been decided not to try to evaluate the efficiency of the lines on the available commissioning data, since a reliable determination would be hard to achieve, because of the preliminary detector performances, significantly overlapping with selection ones.

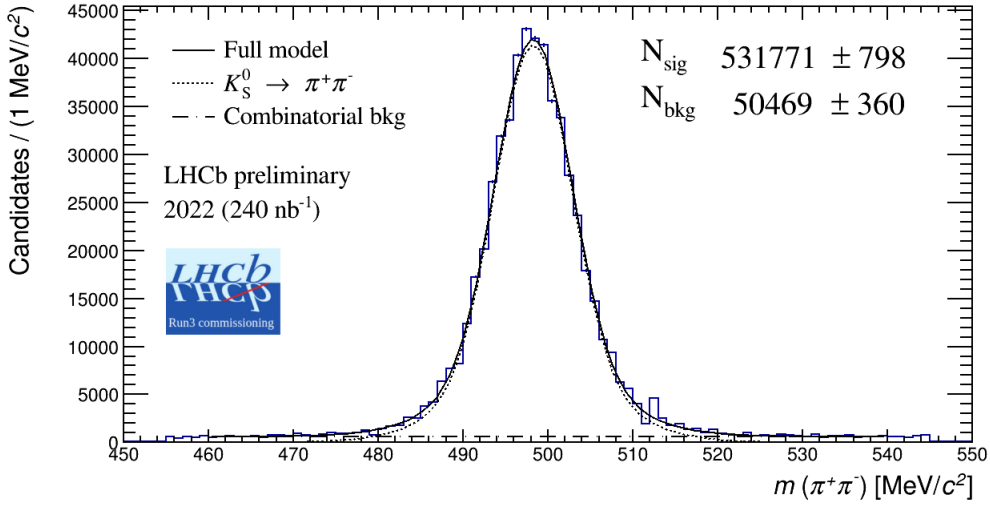


Figure 1: Invariant mass for K_S^0 candidates and collected by TwoTrackKs. Taken from [41].

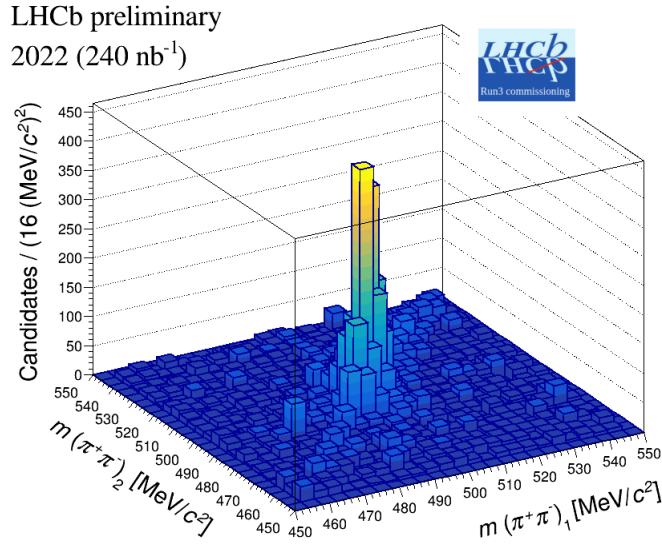


Figure 2: Invariant mass for K_S^0 candidate pairs collected by TwoKs. Taken from [41].

3.2 Rates on real pp collisions

Reliably reproducing generic pp collision on simulation is a challenging task and new selections background acceptance could be significantly higher on real data than expectations, potentially making lines exploitation unfeasible. Therefore, a crucial check is the estimate of lines rate on real data.

Two unfiltered samples have been exploited, collected at different instantaneous luminosity values, here quantified through the parameter μ , the average number of visible pp interactions per bunch crossing. Rates computed at different μ values are reported in Table 2. Measured rates appear

μ	Rate TwoTrackKs [kHz]	Rate TwoKs [kHz]
1.1	1.24 ± 0.08	0.05 ± 0.02
3.1	4.2 ± 0.5	2.5 ± 0.4
5.32 (Simulation)	74 ± 7	13 ± 3

Table 2: TwoTrackKs and TwoKs HLT1 lines rates computed on real data and simulation.

to be well under control, largely below simulations predictions for both considered μ values, despite the growth present when considering higher μ value. The TwoKs line rate shows a steeper rate increase, as expected for a 4-track selection. Data at the nominal LHCb Run 3 luminosity ($\mu = 5.5$) are not available, preventing from a direct comparison with simulation predictions. Nevertheless, this test clearly verifies finiteness of implemented selections rate, demonstrating their feasibility and motivating their exploitation also during Run 3 physics data taking.

4. Possible acceptance extension

The early triggering LLP-dedicated selections here considered demonstrated a significant impact in LLP online selection efficiency. However, their effect is anyway constrained by a major acceptance limitation, hence lack of downstream and T tracks reconstruction at HLT1 level, preventing retention of the significant fraction of LLP decaying outside of the VELO acceptance.

4.1 HLT1 downstream triggering potential

The potential efficiency improvement achievable in case of downstream triggering availability is estimated. A simplified offline HLT1 emulator made of three lines is exploited. Considered lines are: a single-track (1-track) and a two-track (2-track) selection emulating general-purpose LHCb HLT1 lines and a K_S^0 -dedicated one, implementing TwoTrackKs selections. The latter is the only one extended to downstream triggering. In order to estimate efficiency gain and rate cost of acceptance extension, the considered system is run over a set of samples (both real and simulated data). These are reconstructed with an offline-level precision, higher than the one achievable during HLT1 processing. However, it has been decided to ignore this difference, since it is expected to do not have any significant impact, being this a first order estimate.

Efficiency gain when TwoTrackKs line is extended to downstream triggering has been estimated on some representative K_S^0 -final state decays, results are reported in Table 3. Fully K_S^0 -final state decays show the most significant improvement, reaching a factor larger than 5 (3) in case of $B^0 \rightarrow K_S^0 K_S^0$ ($D^0 \rightarrow K_S^0 K_S^0$). It's worth noting how these gains add up to the ones due to the implementation of K_S^0 -dedicated HLT1 line triggering on long tracks only. Therefore, the implementation of a TwoTrackKs-like line, without any acceptance limitation, could determine an efficiency improvement up to a factor 8.5, when considering $D^0 \rightarrow K_S^0 K_S^0$ decays. A less significant efficiency improvement is achieved in case of $K_S^0 \pi^+ \pi^-$ final state decays. This is expected, since the $\pi^+ \pi^-$ pair directly coming from the D^0 efficiently triggers general-purpose single- and two-track selections and the fraction of decays triggered through the K_S^0 is lower in any case. However, in this case

Sample	Efficiency gain factor
$D^0 \rightarrow K_S^0 K_S^0$	3.3
$D^0 \rightarrow K_S^0 \pi^+ \pi^-$	1.14
$B^0 \rightarrow K_S^0 K_S^0$	5.6
$B^0 \rightarrow K_S^0 \pi^+ \pi^-$	1.09

Table 3: Efficiency gain achieved extending TwoTrackKs HLT1 line to downstream reconstructed LLP candidates.

triggering on the final state K_S^0 could prevent the insurgence of major systematic effects during offline analysis, appearing when events are triggered through the $\pi^+ \pi^-$ pair. In this scenario, having the possibility of triggering also on K_S^0 decaying outside VELO is a key factor in order to collect a sizeable statistics sample and the verified efficiency gain is anyway important.

The rate cost of considered downstream trigger configuration is determined exploiting the same HLT1 emulator, ran over a sample of pp collisions collected by LHCb in 2018, scaling estimated rates to Run 3 luminosity. Real data exploitation is preferred in this case, in order to have a more reliable estimate. Results are reported in Table 4. The rate of system given by 1-track and 2-track is

Selections	Rate [kHz]
1-track \vee 2-track	1518 ± 92
1-track \vee 2-track \vee TwoTrackKs (long tracking)	1518 ± 92
1-track \vee 2-track \vee TwoTrackKs (long and downstream tracking)	1767 ± 99

Table 4: Rate estimates in case of downstream tracking availability at HLT1 level.

of the expected order of magnitude ($O \sim 1$ MHz), even if at first order. The addition of TwoTrackKs does not cause any significant increase in the rate at the considered precision level, agreeing with the minimal impact verified on simulation and real data. Rates for these two configurations have been computed as a sanity check. Achieved results suggest a reliable emulation of HLT1 system, indicating the same also when considering downstream tracks. Extension of TwoTrackKs line to downstream triggering determines a limited rate increase, corresponding to 15% of the overall HLT1 system rate. This result strongly suggests feasibility of considered approach, representing a crucial step toward downstream tracking implementation.

4.2 Downstream tracking efforts

Efforts toward the implementation of HLT1 downstream tracking are already ongoing within the LHCb collaboration. Standalone T-tracks reconstruction has been already ported to HLT1, implemented in GPU framework [42], and exploited during data taking. However, this task is very

computationally expensive, occupying $\sim 45\%$ of the overall HLT1 timing budget [42], strongly motivating efforts aimed at reducing this time.

One of the approaches considered in order to speed up T-tracks reconstruction in future LHC runs involves the implementation a dedicated device, performing reconstruction of T-tracks at readout level, before HLT1, investigated by LHCb with an advanced R&D project, named DoWnstream Tracker (DWT) [43]. It targets a 30 MHz forward tracking (SciFi/UT-SciFi) from Run 4, exploiting the so-called RETINA algorithm, implemented on a FPGA-based device. Forward tracks reconstruction is performed before event-building, making track appear as raw data coming out of detector. The implementation of such a device allows HLT1 downstream triggering, and the achievement of aforementioned efficiency gain, while saving a significant amount of processing time both at HLT1 and HLT2 level, making room for the execution of other tasks, as event reconstruction at an earlier trigger stage or the implementation of more channel-specific selections.

5. Conclusions

We presented results from a first example of LLP-dedicated selections working at the earliest trigger level at LHC, targeting the selection of K_S^0 candidates. Promising simulation studies motivated the implementation of these selections in LHCb trigger system and their exploitation at the re-start of LHCb data taking in 2022. First data collected in Run 3 allowed for an early test of these novel lines, showing an affordable rate and a good purity of collected candidates, suggesting their further exploitation in future physics data taking periods.

The results reported here represent an important proof of concept in triggering at hadron-collider experiments, as the illustrated strategy can be extended to other LLP decays, potentially impacting several SM and BSM studies, currently limited by available statistics. This approach also sets an interesting example beyond the LLP realm, of successful channel-specific trigger selections at the very first trigger level. This approach could be fruitfully applied to other kind of selections in future large luminosity scenarios at hadron colliders.

References

- [1] ATLAS collaboration, *Search for long-lived, massive particles in events with displaced vertices and multiple jets in pp collisions at $\sqrt{s} = 13$ TeV with the ATLAS detector*, .
- [2] ATLAS collaboration, *Search for Displaced Leptons in $\sqrt{s} = 13$ TeV pp Collisions with the ATLAS Detector*, *Phys. Rev. Lett.* **127** (2021) 051802 [2011.07812].
- [3] ATLAS collaboration, *A search for the decays of stopped long-lived particles at $\sqrt{s} = 13$ TeV with the ATLAS detector*, *JHEP* **07** (2021) 173 [2104.03050].
- [4] ATLAS collaboration, *Search for long-lived charginos based on a disappearing-track signature using 136 fb^{-1} of pp collisions at $\sqrt{s} = 13$ TeV with the ATLAS detector*, *Eur. Phys. J. C* **82** (2022) 606 [2201.02472].

- [5] ATLAS collaboration, *Search for heavy long-lived multi-charged particles in the full LHC Run 2 pp collision data at $s=13$ TeV using the ATLAS detector*, *Phys. Lett. B* **847** (2023) 138316 [2303.13613].
- [6] ATLAS, CMS collaboration, *Measurements of the Higgs boson production and decay rates and constraints on its couplings from a combined ATLAS and CMS analysis of the LHC pp collision data at $\sqrt{s} = 7$ and 8 TeV*, *JHEP* **08** (2016) 045 [1606.02266].
- [7] D0 collaboration, *Search for Resonant Pair Production of long-lived particles decaying to b anti- b in p anti- p collisions at $s^{*(1/2)} = 1.96$ -TeV*, *Phys. Rev. Lett.* **103** (2009) 071801 [0906.1787].
- [8] CDF collaboration, *Search for heavy metastable particles decaying to jet pairs in $p\bar{p}$ collisions at $\sqrt{s} = 1.96$ TeV*, *Phys. Rev. D* **85** (2012) 012007 [1109.3136].
- [9] ATLAS collaboration, *Search for pair-produced long-lived neutral particles decaying in the ATLAS hadronic calorimeter in pp collisions at $\sqrt{s} = 8$ TeV*, *Phys. Lett. B* **743** (2015) 15 [1501.04020].
- [10] CMS collaboration, *Search for Long-Lived Neutral Particles Decaying to Quark-Antiquark Pairs in Proton-Proton Collisions at $\sqrt{s} = 8$ TeV*, *Phys. Rev. D* **91** (2015) 012007 [1411.6530].
- [11] LHCb collaboration, *Updated search for long-lived particles decaying to jet pairs*, *Eur. Phys. J. C* **77** (2017) 812 [1705.07332].
- [12] R.N. Mohapatra and G. Senjanovic, *Neutrino Mass and Spontaneous Parity Nonconservation*, *Phys. Rev. Lett.* **44** (1980) 912.
- [13] T. Yanagida, *Horizontal gauge symmetry and masses of neutrinos*, *Conf. Proc. C* **7902131** (1979) 95.
- [14] J. Schechter and J.W.F. Valle, *Neutrino Masses in $SU(2) \times U(1)$ Theories*, *Phys. Rev. D* **22** (1980) 2227.
- [15] A.M. Abdullahi et al., *The present and future status of heavy neutral leptons*, *J. Phys. G* **50** (2023) 020501 [2203.08039].
- [16] CMS collaboration, *Search for long-lived heavy neutral leptons with displaced vertices in proton-proton collisions at $\sqrt{s} = 13$ TeV*, *JHEP* **07** (2022) 081 [2201.05578].
- [17] M. Graham, C. Hearty and M. Williams, *Searches for Dark Photons at Accelerators*, *Ann. Rev. Nucl. Part. Sci.* **71** (2021) 37 [2104.10280].
- [18] A. Hook, S. Kumar, Z. Liu and R. Sundrum, *High Quality QCD Axion and the LHC*, *Phys. Rev. Lett.* **124** (2020) 221801 [1911.12364].
- [19] G. D'Ambrosio and T. Kitahara, *Direct CP Violation in $K \rightarrow \mu^+ \mu^-$* , *Phys. Rev. Lett.* **119** (2017) 201802 [1707.06999].

- [20] LHCb collaboration, *Constraints on the $K_S^0 \rightarrow \mu^+ \mu^-$ Branching Fraction*, *Phys. Rev. Lett.* **125** (2020) 231801 [2001.10354].
- [21] LHCb collaboration, *Observation of CP Violation in Charm Decays*, *Phys. Rev. Lett.* **122** (2019) 211803 [1903.08726].
- [22] U. Nierste and S. Schacht, *CP Violation in $D^0 \rightarrow K_S K_S$* , *Phys. Rev. D* **92** (2015) 054036 [1508.00074].
- [23] CLEO collaboration, *Search for CP violation in $D^0 \rightarrow K_S^0 \pi^0$ and $D^0 \rightarrow \pi^0 \pi^0$ and $D^0 \rightarrow K_S^0 K_S^0$ decays*, *Phys. Rev. D* **63** (2001) 071101 [hep-ex/0012054].
- [24] N. Dash et al., *Search for CP Violation and Measurement of the Branching Fraction in the Decay $D^0 \rightarrow K_S^0 K_S^0$* , *Phys. Rev. Lett.* **119** (2017) 171801 [1705.05966].
- [25] LHCb collaboration, *Measurement of the time-integrated CP asymmetry in $D^0 \rightarrow K_S^0 K_S^0$ decays*, *JHEP* **10** (2015) 055 [1508.06087].
- [26] LHCb collaboration, *Measurement of CP asymmetry in $D^0 \rightarrow K_S^0 K_S^0$ decays*, *Phys. Rev. D* **104** (2021) L031102 [2105.01565].
- [27] A.B. Carter and A.I. Sanda, *CP Violation in B Meson Decays*, *Phys. Rev. D* **23** (1981) 1567.
- [28] I.I.Y. Bigi and A.I. Sanda, *Notes on the Observability of CP Violations in B Decays*, *Nucl. Phys. B* **193** (1981) 85.
- [29] BABAR collaboration, *Measurement of Time-Dependent CP Asymmetry in $B^0 \rightarrow c$ anti- c $K^{(*)0}$ Decays*, *Phys. Rev. D* **79** (2009) 072009 [0902.1708].
- [30] BELLE-II collaboration, *Measurement of decay-time-dependent CP violation in $B^0 \rightarrow J/\psi K_S^0$ decays using 2019-2021 Belle II data*, [2302.12898](#).
- [31] LHCb collaboration, *Measurement of CP Violation in $B^0 \rightarrow \psi(\rightarrow \ell^+ \ell^-) K_S^0(\rightarrow \pi^+ \pi^-)$ Decays*, *Phys. Rev. Lett.* **132** (2024) 021801 [2309.09728].
- [32] ICECUBE collaboration, *Icecube - the next generation neutrino telescope at the south pole*, *Nucl. Phys. B Proc. Suppl.* **118** (2003) 388 [astro-ph/0209556].
- [33] SUPER-KAMIOKANDE collaboration, *The Super-Kamiokande detector*, *Nucl. Instrum. Meth. A* **501** (2003) 418.
- [34] NA62 collaboration, *The Beam and detector of the NA62 experiment at CERN*, *JINST* **12** (2017) P05025 [1703.08501].
- [35] G. Aielli et al., *Expression of interest for the CODEX-b detector*, *Eur. Phys. J. C* **80** (2020) 1177 [1911.00481].
- [36] FASER collaboration, *FASER: ForwArd Search ExpeRiment at the LHC*, [1901.04468](#).

- [37] M. Benedikt, A. Blondel, O. Brunner, M. Capeans Garrido, F. Cerutti, J. Gutleber et al., *Future Circular Collider - European Strategy Update Documents*, 2019.
- [38] LHCb collaboration, *The LHCb upgrade I*, [2305.10515](#).
- [39] LHCb collaboration, *A Comparison of CPU and GPU Implementations for the LHCb Experiment Run 3 Trigger*, *Comput. Softw. Big Sci.* **6** (2022) 1 [[2105.04031](#)].
- [40] H. Voss, A. Hoecker, J. Stelzer and F. Tegenfeldt, *TMVA - Toolkit for Multivariate Data Analysis with ROOT*, *PoS ACAT* (2007) 040.
- [41] LHCb collaboration, *HLT1 TwoTrackKs and TwoKs lines invariant mass plots*, *LHCb-FIGURE-2023-005* (2023) .
- [42] LHCb-RTA collaboration, *Effect of the high-level trigger for detecting long-lived particles at LHCb*, *Front. Big Data* **5** (2022) 1008737.
- [43] LHCb collaboration, *Real-time reconstruction of long-lived particles at LHCb using FPGAs*, *J. Phys. Conf. Ser.* **1525** (2020) 012101 [[2006.11067](#)].